E.J. Brash,[1,*] A. Kozlov,[1] Sh. Li,[1] G.M. Huber,[1]
[1] *University of Regina, Regina, Saskatchewan, Canada, S4S 0A2*
(November 13, 2001)

Recent measurements of the ratio of the elastic electromagnetic form factors of the proton, G_{Ep}/G_{Mp}, using the polarization transfer technique at Jefferson Lab show that this ratio decreases dramatically with increasing Q^2, in contradiction to previous measurements using the Rosenbluth separation technique. Using this new high quality data as a constraint, we have reanalyzed most of the world *ep* elastic cross section data. In this paper, we present a new empirical fit to the reanalyzed data for the proton elastic magnetic form factor in the region $0 < Q^2 < 30\ GeV^2$. As well, we present an empirical fit to the proton electromagnetic form factor ratio, G_{Ep}/G_{Mp}, which is valid in the region $0.1 < Q^2 < 6\ GeV^2$.

The elastic electromagnetic form factors are crucial to our understanding of the proton's internal structure. Indeed, the differential cross section for elastic $ep \rightarrow ep$ scattering is described completely in terms of the Dirac and Pauli form factors, F_1 and F_2, respectively, based solely on fundamental symmetry arguments. Further, the Sachs form factors, G_{Ep} and G_{Mp}, which are simply derived from F_1 and F_2, reflect the distributions of charge and magnetization current within the proton.

Until recently, these form factors have been determined experimentally using the Rosenbluth separation method [3], in which one measures elastic *ep* cross sections at constant Q^2, and varies both the beam energy and scattering angle to separate the electric and magnetic contributions. In terms of the Sachs form factors, the differential cross section for elastic *ep* scattering is written as

$$\frac{d\sigma}{d\Omega} = \sigma_{ns}\left(\frac{G_{Ep}^2 + \tau G_{Mp}^2}{1+\tau} + 2\tau G_{Mp}^2 tan^2(\theta_e/2)\right), \tag{1}$$

where $\tau = Q^2/4M_p^2$, θ_e is the in-plane electron scattering angle, and σ_{ns} is the nonstructure cross section. In practice, one typically derives a "reduced cross section", defined according to

$$\sigma_R = \frac{d\sigma}{d\Omega}\frac{(1+\tau)\epsilon}{\sigma_{ns}\tau} = \frac{\epsilon}{\tau}G_{Ep}^2(Q^2) + G_{Mp}^2(Q^2), \tag{2}$$

where $\epsilon = \{1 + 2(1+\tau)tan^2(\theta_e/2)\}^{-1}$ is a measure of the virtual photon polarization. Equation 2 is known as the Rosenbluth formula, and shows that fits to reduced cross section measurements made at constant Q^2 but varying ϵ values may be used to extract both form factors independently.

It is interesting to note, however, that with increasing Q^2, the reduced cross sections are increasingly dominated by the magnetic term G_{Mp}; at $Q^2 \approx 3\ GeV^2$, the electric term contributes only a few percent of the cross section. Furthermore, referring to the open data points in the left panel of Fig. 1, one can see that the various Rosenbluth separation data sets [4–10] for the ratio $\mu G_{Ep}/G_{Mp}$ are not consistent with one another for $Q^2 > 1\ GeV^2$. Thus, while it is clear that a tremendous effort has gone into the analysis of these difficult experiments, one is forced to conclude that some of the experiments have underestimated the systematic errors.

Due to the fundamental nature of the quantities at hand, a more robust method for measuring the proton electromagnetic form factors is certainly desirable. Over the last few years, focal plane polarimeters have been installed in hadron spectrometers in experimental facilities at Bates, Mainz, and Jefferson Lab. Specifically, one makes use of the polarization transfer method [11,12], in which one measures, using a focal plane polarimeter, the transverse (P_t) and longitudinal (P_ℓ) components of the recoil proton polarization in $^1H(\vec{e}, e'\vec{p})$ scattering, using a longitudinally polarized electron beam.

Interestingly, the proton form factor ratio is given simply by

$$r = \mu\frac{G_{Ep}}{G_{Mp}} = -\frac{P_t}{P_\ell}\frac{\mu\,(E_e + E_{e'})}{2M_p}\tan(\theta_e/2)\,. \tag{3}$$

Here, E_e ($E_{e'}$) is the incident (scattered) electron energy. The polarization transfer method offers a number of advantages over the traditional Rosenbluth separation technique. Using the ratio of the two simultaneously measured polarization components greatly reduces systematic uncertainties. For example, a detailed knowledge of the spectrometer acceptances, something which plagues the cross section measurements, is in general not needed. Moreover, it is not necessary to know either the beam polarization or the polarimeter analyzing power, since both of these quantities

cancel in measuring the ratio of the form factors. The dominant systematic uncertainty is the knowledge of spin transport, although in comparison to the size of the systematic uncertainties in cross section measurements, this too is small.

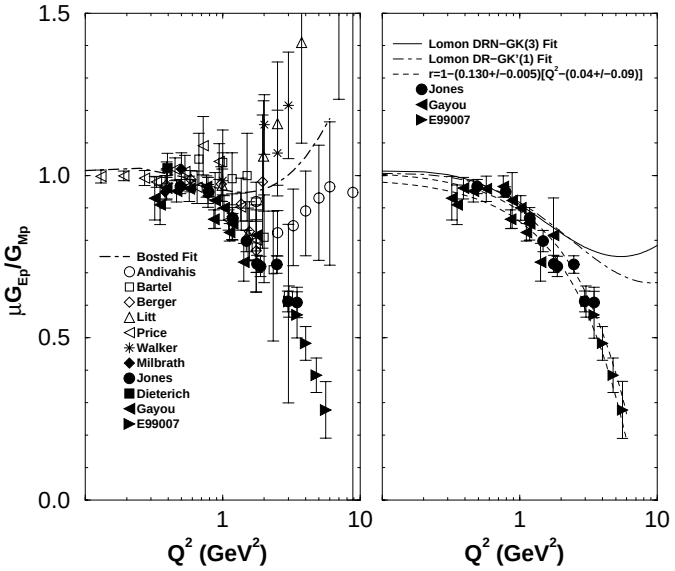

FIG. 1. (a) Published world data for $r = \mu_p G_{Ep}/G_{Mp}$; open symbols indicate Rosenbluth separations [4–10] while filled symbols indicate polarization transfer measurements [1,2,13–15]. The dot dash line is the parameterization from ref. [16] to the cross section data, which indicates $r \approx 1$. (b) Fit to polarization transfer measurements from Jefferson Lab. Included are the most recent data at large Q^2 from E99007 [2]. Also shown are calculated ratios from recent fits to the electromagnetic form factors by Lomon [17] within the Gari-Krümpelmann framework.

As mentioned above, the proton form factor ratio has been measured at several facilities using the polarization transfer technique. It was first used by Milbrath *et al.* [13], who determined r at $Q^2 = 0.38$ and 0.50 GeV^2, and the result was in good agreement with both the Rosenbluth separation results and a subsequent polarization measurement at $Q^2 = 0.4$ by Dieterich *et al.* [14] at Mainz. However, polarization transfer measurements up to Q^2=3.5 GeV^2 in Hall A at Jefferson Lab [1,15] have revealed the somewhat surprising result shown in Fig. 1, that the form factor ratio decreases with increasing Q^2. Most recently, this trend has been confirmed in Jefferson Lab Experiment E99007 [2], which extends the form factor ratio measurement to Q^2=5.6 GeV^2; these new data are also shown in Fig. 1. We have fit the Jefferson Lab data using a simple linear parameterization, i.e.,

$$r = 1.0 - (0.130 \pm 0.005)\left[Q^2 - (0.04 \pm 0.09)\right], \tag{4}$$

for $0.04 < Q^2 < 5.6$ GeV^2. This empirical description, which gives an acceptable fit to the Jefferson Lab data with the smallest number of free parameters, is shown in the right panel of Fig. 1 using two dashed curves to represent the range of uncertainty in the fit parameters. Note that this description of the ratio is singularly inconsistent with the global fit from Ref. [16] shown in the left panel of Fig. 1. However, a similar decreasing ratio has been reported in a number of recent theoretical models. In addition, we also show in the right panel of Fig. 1 ratios calculated from recent fits to the electromagnetic form factors by Lomon [17] within the framework of the Gari-Krümpelmann model. The two curves shown differ somewhat from one another in their specific choice of the form of the hadronic form factors as well as in the parametrization of the behaviour at large Q^2, and as such represent upper and lower bounds on the extracted form factor ratio. We note, however, that these curves both lie significantly above the new data.

In the remainder of this paper, for the purposes of reanalyzing the cross section data, we have used an empirical prescription for the form factor ratio. For $Q^2 < 0.04$ GeV^2, we have used $r = 1$; for $0.04 < Q^2 < 7.7$ GeV^2, we have employed Eq. 4; for $Q^2 > 7.7$ GeV^2, we have used $r = 0$. The boundary of 0.04 GeV^2 (7.7 GeV^2) corresponds to the value of Q^2 where Eq. 4 predicts a ratio of 1 (0). The choice of setting $r = 0$ for the largest Q^2 region is somewhat arbitrary, since no experimental data exists in this kinematic regime. However, since the electric contribution to the total cross section is minimal in this Q^2 region, our choice has in fact little impact on the extracted value of the magnetic form factor. In addition, our linear fit almost certainly has the wrong asymptotic behavior at very large Q^2,

based on theoretical expectations, and therefore we have extended the empirical fit only to Q^2=7.7 GeV^2 to match the higher Q^2 assumption of $r = 0$.

As stated above, the new Jefferson Lab data for the form factor ratio is in general disagreement with the higher Q^2 Rosenbluth separation measurements. Since the Rosenbluth separation measurements systematically attribute more strength in the cross section to the electric part (larger ratio, r), this means that their extracted values for the magnetic form factor, G_{Mp}, are potentially systematically too small.

We have reanalyzed the available cross section data using the following procedure:

- In the cases where experiments have extracted reduced cross section data at multiple ϵ values at each Q^2 (Refs. [4–10]), we have reanalyzed this data using the aforementioned form factor ratio prescription. The net effect of this procedure is that the form factor ratio constraint fixes the ratio of the slope to the intercept of the graph of reduced cross section vs. ϵ. Therefore, in practice, one extracts only a single parameter from the new fit to the data.

- For the data of Sill *et al.* [18], which presents reduced cross section data at a single ϵ value for each Q^2, we extract G_{Mp} using the above form factor ratio prescription directly. Note that the authors had assumed, quite reasonably at the time, $r = 1$ in their extraction of G_{Mp}.

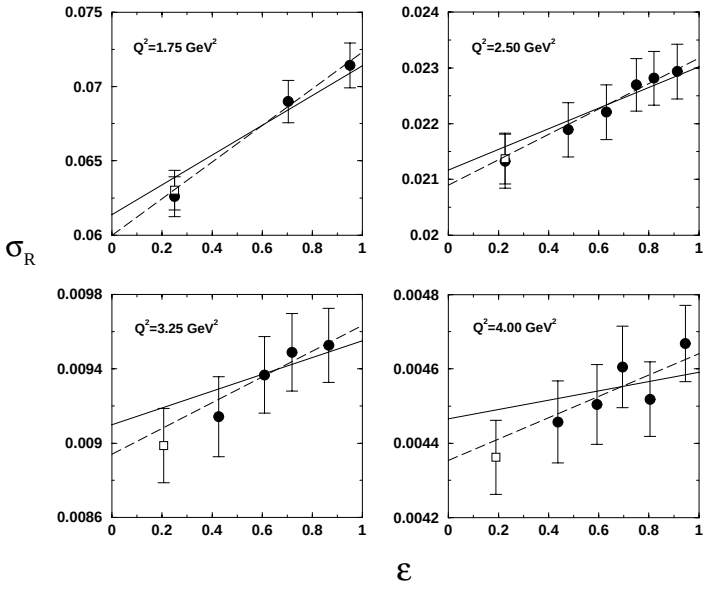

FIG. 2. The reduced cross section data of Andivahis *et al.* for the four lowest Q^2 values of 1.75, 2.50, 3.25, and 4.0 GeV^2. The fits are explained in the text.

As an example of the effect of form factor ratio constraint, in Fig. 2, we show the reduced cross section data from Andivahis *et al.*, for the four lowest Q^2 values of 1.75, 2.50, 3.25, and 4.0 GeV^2. In each case, the dashed line is the best fit line using the direct Rosenbluth method. The solid line is the best fit using our form factor ratio constraint. The error bars shown are statistical and point-to-point systematic errors, as reported in Ref. [4], added in quadrature. In this paper, the authors also report an overall normalization uncertainty of $\delta_{norm} = 1.77\%$. We have not included this uncertainty in each data point, but it has been included in the final uncertainty in the intercept of each graph, as

$$(\delta b_{final})^2 = (\delta b_{raw})^2 + (b_{raw} \cdot \delta_{norm})^2, \tag{5}$$

where b_{raw} is the intercept of the straight-line fit to the data. In addition, in the final extraction of G_{Mp} using the form factor ratio constraint, we have incorporated (in quadrature) the uncertainty in the form factor ratio itself, as expressed in Eq. 4. The results of the two extraction methods, including the final uncertainties, are summarized in Tab. I.

TABLE I. Compilation of all $\frac{G_{M_p}}{\mu_p G_D}$ extraction results

Q^2 (GeV^2)	Direct Extraction	New Extraction	Q^2 (GeV^2)	Direct Extraction	New Extraction
	Andivahis *et al.* [4]			Berger *et al.* [6]	
1.750	1.0528 ± 0.013	1.0670 ± 0.010	0.389	0.9861 ± 0.027	0.9873 ± 0.021
2.500	1.0579 ± 0.012	1.0662 ± 0.010	0.584	0.9865 ± 0.022	1.0038 ± 0.021
3.250	1.0532 ± 0.015	1.0633 ± 0.010	0.779	1.0071 ± 0.024	1.0174 ± 0.021
4.000	1.0397 ± 0.015	1.0535 ± 0.010	0.973	1.0080 ± 0.026	1.0384 ± 0.022
5.000	1.0277 ± 0.015	1.0354 ± 0.010	1.168	1.0275 ± 0.031	1.0548 ± 0.023
6.000	1.0017 ± 0.019	1.0118 ± 0.011	1.363	1.0417 ± 0.030	1.0483 ± 0.023
7.000	0.9734 ± 0.022	1.0022 ± 0.013	1.558	1.0359 ± 0.035	1.0665 ± 0.024
	Bartel *et al.* [5]		1.752	1.0685 ± 0.042	1.0712 ± 0.025
0.670	0.9659 ± 0.028	1.0082 ± 0.014		Janssens *et al.* [10]	
1.000	1.0170 ± 0.028	1.0587 ± 0.015	0.156	0.9259 ± 0.027	0.9789 ± 0.013
1.169	1.0202 ± 0.024	1.0556 ± 0.014	0.179	0.9598 ± 0.016	0.9686 ± 0.009
1.500	1.0350 ± 0.030	1.0697 ± 0.015	0.195	1.0016 ± 0.026	0.9981 ± 0.013
1.750	1.0562 ± 0.023	1.0565 ± 0.015	0.234	0.9379 ± 0.025	0.9854 ± 0.011
3.000	1.0581 ± 0.023	1.0587 ± 0.014	0.273	0.9403 ± 0.017	0.9620 ± 0.009
	Litt *et al.* [7]		0.292	0.9347 ± 0.020	0.9663 ± 0.009
1.500	0.9757 ± 0.115	1.0749 ± 0.022	0.312	0.9669 ± 0.016	0.9662 ± 0.009
2.000	0.9835 ± 0.075	1.0755 ± 0.022	0.350	0.9744 ± 0.025	0.9745 ± 0.012
2.500	1.0169 ± 0.035	1.0699 ± 0.022	0.389	0.9590 ± 0.014	0.9843 ± 0.008
3.750	0.9779 ± 0.041	1.0795 ± 0.022	0.428	0.9704 ± 0.024	0.9990 ± 0.012
	Sill *et al.* [18]		0.467	0.9779 ± 0.016	0.9957 ± 0.009
2.862	1.0228 ± 0.018	1.0627 ± 0.021	0.506	0.9585 ± 0.024	0.9900 ± 0.012
3.621	1.0237 ± 0.020	1.0600 ± 0.023	0.545	0.9879 ± 0.016	1.0029 ± 0.009
5.027	1.0070 ± 0.018	1.0401 ± 0.019	0.584	0.9838 ± 0.024	1.0045 ± 0.012
4.991	1.0110 ± 0.019	1.0425 ± 0.021	0.623	0.9913 ± 0.016	0.9986 ± 0.009
5.017	1.0000 ± 0.018	1.0270 ± 0.019	0.662	1.0305 ± 0.025	1.0193 ± 0.012
7.300	0.9494 ± 0.019	0.9732 ± 0.020	0.701	0.9864 ± 0.017	1.0117 ± 0.009
9.629	0.8906 ± 0.019	0.9071 ± 0.020	0.740	1.0198 ± 0.025	1.0419 ± 0.012
11.99	0.8729 ± 0.019	0.8855 ± 0.020	0.779	1.0396 ± 0.018	1.0259 ± 0.009
15.72	0.8206 ± 0.026	0.8291 ± 0.025	0.857	1.0888 ± 0.018	1.0709 ± 0.011
19.47	0.7323 ± 0.028	0.7381 ± 0.029			
23.24	0.7292 ± 0.033	0.7338 ± 0.033			
26.99	0.7099 ± 0.041	0.7131 ± 0.042			
31.20	0.7211 ± 0.064	0.7230 ± 0.064			

In Fig. 3, we show data for the proton magnetic form factor, expressed as $G_{Mp}/\mu G_D$, where $G_D = (1+Q^2/0.71)^{-2}$ is the dipole form factor parameterization. In the left panel, we show the magnetic form factor as extracted using direct Rosenbluth separation (or using the assumption of $r = 1$ in the case of the data of Sill *et al.*). In the right panel, we show the newly extracted data using the above constraint on the form factor ratio. In both panels, the dashed curve is the parameterization of Bosted [16], while in the right panel, the solid line is our new empirical fit, and is given by

$$\frac{G_{Mp}}{\mu} = \frac{1}{1 + (0.126 \pm 0.064)Q + (2.849 \pm 0.145)Q^2 + (0.235 \pm 0.100)Q^3 + (1.016 \pm 0.076)Q^4 + (0.343 \pm 0.022)Q^5}, \tag{6}$$

the form of which is consistent with Ref. [16].

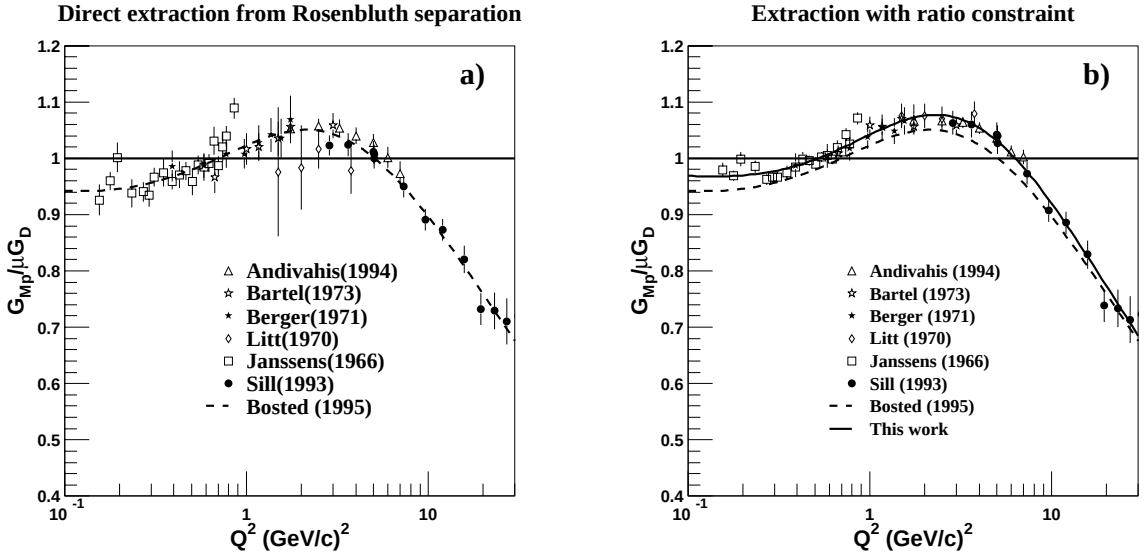

FIG. 3. a) The proton magnetic form factor, expressed as $G_{Mp}/\mu G_D$, as published in the literature. b) The proton magnetic form factor, after reanalysis using the form factor ratio constraint. The solid line is the new empirical fit, as explained in the text, while the dashed line is the parameterization from Ref. [16].

Imposing the form factor ratio constraint has the expected effect that the extracted magnetic form factor is systematically larger than when one uses the direct Rosenbluth method. Indeed, the data in the right panel of Fig. 3 lie approximately 1.5-3% above the Bosted parameterization. As mentioned earlier, the decreased electric strength implicit in a decreasing form factor ratio results in increased magnetic strength. However, perhaps the most striking feature of the reanalyzed data is that imposing the constraint on the form factor ratio results in uncertainties that are much reduced compared to using the direct Rosenbluth separation. This is due simply to the fact that we are extracting only a single parameter (proportional to G_{Mp}) from the cross section data, as opposed to extracting two parameters, as is done with the Rosenbluth method. We note also that the Bosted parameterization and our new fit converge at large Q^2. As stated previously, the electric strength at large Q^2 decreases rapidly, and so indeed our choice of $r = 0$, compared to the previous choice of $r = 1$, has little effect on the magnetic form factor extracted from the data of Sill *et al.*

One also sees immediately that in using the new form factor constraint, the extracted magnetic form factor data from the various experiments are more consistent with one another, as well as with the new parameterization. Comparing the data extracted using direct Rosenbluth separation to the Bosted parameterization, we calculate $\chi^2/N_{d.f.}$=0.97. Note that this is somewhat larger than the value quoted in Ref. [16], since we have used a different data sample. Using the form factor constraint, and comparing to our new parameterization, $\chi^2/N_{d.f.}$=0.85.

Based on our new parameterizations of both G_{Mp} and the form factor ratio, we may calculate the elastic hydrogen differential cross section directly using Eq. 1. In Fig. 4, we show the deviation of the cross section calculated using the new fits from the measured world cross section data [4–10] as a function of Q^2. The deviations form an approximately Gaussian distribution around zero, with a standard deviation of $\sim$2.5%.

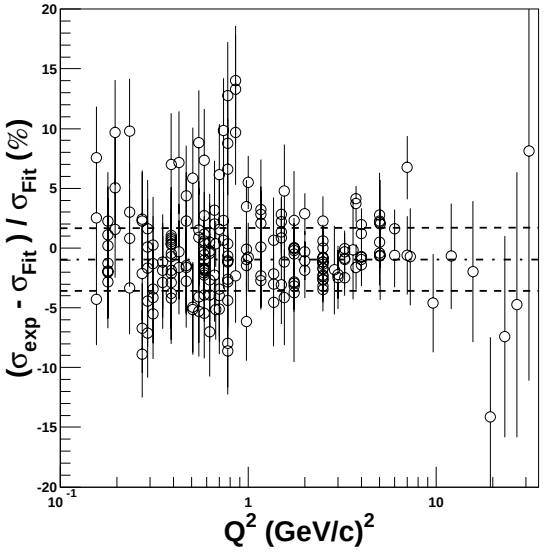

FIG. 4. Deviations of the elastic hydrogen differential cross section calculated with new parametrizations of G_{Mp} and the form factor ratio (σ_{Fit}) from data [4–10] published in the literature (σ_{exp}).

In conclusion, we have used recent measurements of the ratio of the elastic electromagnetic form factors of the proton, G_{Ep}/G_{Mp}, using the polarization transfer technique as a constraint in reanalyzing most of the world *ep* elastic cross section data. We have presented a new empirical fit to the reanalyzed data for the proton elastic magnetic form factor in the region $0 < Q^2 < 30\ GeV^2$, and find that over most of this kinematic region, the magnetic form factor is systematically 1.5-3% larger than had been extracted in previous analyses.

This work was supported by the Natural Sciences and Engineering Research Council of Canada.

---

* Corresponding author. Email: brash@uregina.ca

[1] M.K. Jones *et al.*, Phys. Rev. Lett. **84**, 1398 (2000), V. Punjabi *et al.*, to be submitted to Phys. Rev. C.
[2] O Gayou *et al.*, submitted to Phys. Rev. Lett., October, 2001.
[3] M.N. Rosenbluth, Phys. Rev. **79**, 615 (1950).
[4] L. Andivahis *et al.*, Phys. Rev. D **50**, 5491 (1994).
[5] W. Bartel *et al.*, Nucl. Phys. B **58**, 429 (1973).
[6] Ch. Berger *et al.*, Phys. Lett. B **35**, 87 (1971).
[7] J. Litt *et al.*, Phys. Lett. B **31**, 40 (1970).
[8] L.E. Price *et al.*, Phys. Rev. D **4**, 45 (1971).
[9] R.C. Walker *et al.*, Phys. Rev. D **49**, 5671 (1994).
[10] T. Jannsens *et al.*, Phys. Rev. **142**, 922 (1966).
[11] A.I. Akhiezer and M.P. Rekalo, Sov. J. Part. Nucl. **3**, 277 (1974).
[12] R.G. Arnold, C.E. Carlson, and F. Gross, Phys. Rev. C **23**, 363 (1981).
[13] B. Milbrath *et al.*, Phys. Rev. Lett. **80**, 452 (1998), Phys. Rev. Lett. **82**, 2221(E) (1999).
[14] S. Dieterich *et al.*, Phys. Lett. B **500**, 102 (2001).
[15] O. Gayou *et al.*, Accepted for publication in Phys. Rev. C, September 1, 2001.
[16] P.E. Bosted, Phys. Rev. C **51**, 409 (1995).
[17] Earle L. Lomon, Phys. Rev. C **64**, 035204 (2001).
[18] A.F. Sill *et al.*, Phys. Rev. D **48**, 29 (1993).